International Journal of Applied and Natural Sciences
ISSN: 3005-3471
DOI: 10.61424/ijans
Journal Homepage: www.bluemarkpublishers.com/index.php/IJANS

IJANS
BLUEMARK PUBLISHERS

| RESEARCH ARTICLE

Structural Simulation Analysis of the Developed Hybrid of Aluminum Composites and Carbon Nanotube Brake Disc

Vincent Chukwuemeka Ezechukwu[1] ✉ Tamunonimim Kelsy Braide[2], 1feanyi Ugochukwu Onyenanu[3], Gabriel Ayadinuno[4], Joesph Okwudili Agwaziam[5] and Charles Okechukwu Ojinekeya[6]
[123456]Department of Mechanical Engineering, Chukwuemeka Odumegwu Ojukwu University, Anambra State, Nigeria
Corresponding Author: Vincent Chukwemeka Ezechukwu, **E-mail**: vc.ezechukwu@coou.edu.ng

| ABSTRACT
Modifications to the mechanical properties of composite materials are always desired and also widely used in the manufacturing sector due to their weight, superior strength-to-weight ratio, better fracture toughness, improved fatigue, and tensile properties, enhanced corrosion resistance to harsh environments, etc. This study proposed a multiscale finite element (FE) analytical approach to investigate the mechanical behavior of Developed Aluminum Composites Brake Disc using Waste Aluminum Beverage Can, Carbon Nanotube-Derived from Rice Husk (CNTs-derived RH), and Periwinkles Shell Nanoparticles (PWSnp). Based on the experimental findings, it was observed that the maximum stress of the brake disc during the braking process is 15.8402MPa, and the compressive strength of the brake disc is 410MPa. The comparison of the experimental results with the numerical and experimental methods in the literature yielded satisfactory agreements and demonstrated the appropriateness of the composite mechanical behavior for each percentage of CNT weight.

| KEYWORDS

Mechanical strength, Composite, Finite element method, AL-CNT composite, Taguchi-Grey approach.

| ARTICLE INFORMATION

ACCEPTED: 11 January 2025 **PUBLISHED:** 10 February 2025 **DOI:** 10.61424/ijans.v3.i1.195

1. Introduction

Throughout human history, composite materials have been crucial, from the construction of the earliest structures to the development of modern technologies. Our everyday lives have been impacted by composites. The goal of the process is to create a composite material with the desired qualities [Onyenanu, 2024]. The remarkable physiochemical features of carbon nanotubes (CNTs), such as their low density, superior mechanical, electrical, and thermal capabilities, and low coefficient of friction, have garnered significant interest in recent decades and can be used as a reinforcing material. [Braide, 2023, Ezechukwu, 2020].

The application of nanotechnology is one way to enhance and strengthen composite materials. Weight reduction and component reliability are ranked as the most crucial factors in automotive components worldwide today [Onyenanu, 2021]. One of the best options for lightweight materials is aluminum and its alloys because they reduce fuel consumption and emissions, which have a great impact on our ecosystem [Braide, 2022]. Automotive disc brakes are subjected to strong mechanical force, thermal stress, and extreme wear. In the study, [Ezechukwu, 2025] stated that due to its superior wear and heat transfer coefficient, cast iron has historically been one of the more traditional materials used to make brake discs. The shape of graphite is altered by alloying cast iron, which

significantly impacts brake disc wear. Nonetheless, research and development into aluminum matrix composites is driven by the high weight of cast iron and the high cost of the alloying element in order to get beyond these limitations [Ezechukwu, 2020; Nnaji, 2024].

The production of a new nanocomposite material was optimized by Braide et al. [2024] using carbon nanotubes (CNTs) made from rice husks, nanoparticles from periwinkle shells, and Al-Si-Mg alloy made from used beverage cans. Using the Taguchi approach, Nondominated Sorting Genetic Algorithm-II (NSGA-II), and Artificial Neural Networks (ANN), the novel composite's porosity, hardness, and compressive strength were optimized from multiple perspectives. The Taguchi-grey relational methodology was used to optimize the composite's production parameters at the same time. The ideal parameters were 1.5 weight percent CNTs, 1.0 weight percent PWSnp, 100 rpm stirring speed, and 6 minutes of stirring time. The corresponding porosity, hardness, and compressive strength values were 0.3250, 108.2738, and 410.6436. With correlation coefficients of 0.9617, 0.9536, and 0.9725 for the composite material's porosity, hardness, and compressive strength, respectively, the ANN showed exceptional prediction power. Next, multi-objective optimization for the novel material's porosity, hardness, corrosion resistance, and compressive strength was carried out using the ANN as a fitness function within NSGA-II. Using the beneficial qualities of the new material, engineers designing the best brake discs and other machine parts can use the resultant Pareto optimal solutions and the ideal manufacturing settings as a useful resource.

Dhanalakshmi (2018) conducted research on the optimization of aluminum metal matrix composite (AMMC) for use in automobile brake discs. The results showed that graphite had an impact on the wear rate, and silicon carbide had a significant impact on the various mechanical parameters. Gajalakshmi et al. [2022] applied the Taguchi-Grey approach to calculate the wear and coefficient of friction of A6025. Taguchi's design of experiments via the L16 Orthogonal Array was used. The pin-on disc wear technique was applied. They found that the ideal parameters that produced the lowest coefficient of friction, wear, and frictional force were a 111.53 mm disc diameter, 376 r/min disc speeds, and a 35.21 N applied load.

A mechanical device called a brake uses energy from a moving system to stop motion. Usually achieved through friction, it is used to slow or halt a moving wheel, axle, or vehicle or to stop its motion altogether. In order to carry out this job, the brakes absorb the moving member's kinetic strength as well as the potential energy released by objects being lowered via hoists, elevators, and other devices. Heat is released as a result of the energy used to apply brakes [Ezechukwu, 2024, Ezechukwu, 2024]. The work done in this paper can serve as the foundation for the micro mechanism analysis and optimal design of hybrid reinforced composites in the future. A finite element model is used to analyze the strengthening effect and damage effect of adding a reinforcing phase to hybrid reinforced aluminum matrix composites.

2. Materials and method

2.1 Materials

The periwinkle shells used in this study were bought from a local market in Port Harcourt, a major port city in River State, Southern Nigeria, and the rice husks came from Ebonyi State, which is in Southern Nigeria.

2.2 Method

2.2.1 The production of the CNTs from the rice husk waste

Ferrocene, Fe(C5H5)2, as a catalyst, was dissolved in ethanol, and the dried Rice Husk (RH) was added. The mixture was then placed in an aluminum sheet as a substrate. The process of producing CNTs from rice husk waste was carried out according to the procedure used by [Obinwa, 2024]. The RH was cleaned and dried to remove the impurities, and it was then dried at 65 °C for 24 hours. Prior to microwave plasma irradiation, the quartz tube was evacuated into a base pressure of 1.3 × 103 mbar and a deposition time of 40 minutes. The samples were placed in the center of the quartz tube inside the microwave oven (Samsung M539 MAN200405W), 600 W power, and 2.45 GHz frequency (household microwave frequency). The PWSnp was produced using the sol–gel process. The antecedent is the periwinkle shell (PWS). Deionized water was also used to wash the PWS waste. The PWSnp's production details were discussed in another study [Onyenanu, 2021]. The nanocomposites were produced using

the liquid technique of the metal matrix. A graphite crucible containing the cleaned, determined amount of aluminum beverage, 7 wt% Si, and 0.3 wt% Mg was heated to 750°C. In order to increase wettability and balance the temperature, the reinforcement particles, 1.5 wt% PWSnp, and 0.5 wt% RH produced from CNTs were warmed at 1050 °C before being added to the melt. To lessen porosity, degassing tablets (hexachloroethane) were applied once the molten metal had completely melted. A stirrer made of graphite covered in stainless steel was progressively dropped into the melt to stir the molten metal. Five minutes of stirring time and 250 rpm of stirring speed were employed. After that, the molten metal was poured into a mold that had been heated to 30 minutes at 500 °C to achieve homogenous solidification.

2.2.2 The orthogonal array selection

The experimentation in the study was carried out using the L9 orthogonal array. According to the thorough literature studies [Venkatachalam, 2017; Natarajan, 2006], porosity had an impact on the stir cast composite because of the segregation and agglomeration that may happen as a result of increasing the reinforcement, vigorously stirring, and heating the reinforcement particles. The porosity and mechanical characteristics of the final composites are significantly impacted by these processing parameters. The ideal circumstances yield the highest compressive strength, greatest hardness, and minimal porosity.

As indicated in Tables 1 and 2, nine (9) experimental runs were chosen for the L9 orthogonal array by allocating eight columns.

Table 1: Stir casting parameters and their values at a different level

Process parameters	Low (1)	Medium(2)	High(3)
wt%CNTs-derived RH(A),	0.5	1.0	1.5
wt%PWSnp(B)	0.5	1.0	1.5
stirring speed(C) rpm	100	200	300
Stirring time(minutes)	2	4	6

Table 2: Assignment of process parameters using L9 design

%wtCNTs	%wtPWSnp	Stiring speed	Stiring time	Porosity(%)	Hardness Values(HV)	Compressive strength(MPa)
1	1	1	1	0.12	87.56	245.67
1	2	2	2	0.12	89.01	268.23
1	3	3	3	0.15	91.50	289.45
2	1	2	3	0.18	98.32	345.78
2	2	3	1	0.25	99.26	367.8
2	3	1	2	0.34	97.90	355.89
3	1	3	2	0.3	105.89	401.89
3	2	1	3	0.290	116.8	410.67
3	3	2	1	0.30	100.89	398.76

2.2.3 Production of Samples

The liquid method of the metal matrix was employed in the production, which is more dependable and less expensive than another way. The samples were made in accordance with Taguchi's approach of L9 utilizing the Stir casting parameters and their values at a different level, as shown in Table 2. After the molten metal was completely melted, degassing tablets (hexachloroethane) were added to reduce porosity. The cleaned, calculated amount of aluminum beverage, 7wt%Si, and 0.3wt%Mg to form A356 alloy were placed inside a graphite crucible and heated to 750°C. The reinforcement particles were preheated in Table 2 before being incorporated into the melt to improve wettability and harmonize the temperature. To achieve uniform solidification, a stirrer made of stainless steel-coated graphite was used, which was lowered slowly into the melt to stir it according to Table 2. After adding

0.3wt% magnesium to the melted metal, the mixture was poured into a mold that had been preheated to 500°C for 30 minutes. The sample was machined to ascertain its mechanical and physical characteristics after casting.

2.2.4 Production of Prototype Brake Disc

The composites for the brake disc were made using the sand-stir casting method. The composites created under ideal conditions were contrasted with those made for brake disc applications [Venkatachalam, 2017]. The developed composites have been shown to compare favorably with composites developed by [Venkatachalam, 2017, Natarajan, 2006]. The produced composite brake is shown in Figure 1

Figure 1: the produced brake disc

3. Results and discussion

3.1 Multi-response optimization (Grey Analysis).

Table 3 presents the multi-response data from the Taguchi L9, which were analyzed using grey relational analysis to determine the ideal parameter setting that yields higher compressive strength, higher hardness values, and lower porosity. In order to represent the three output characterizations, a single optimal configuration must be obtained using equation 1, where the lower the porosity output characterisation, the better, and the higher the compressive strength and hardness values in equation 2, i.e., 0 ≤ S/N ≤ 1.

$$X_i(k) = \frac{\max X(k)_i - X(k)_i}{\max X_i(k) - \min X(K)_i} \quad (1)$$

$$X_i(K) = \frac{X_i(K) - \min X(K)_i}{\max X - \min X_{Ii}(K)} \quad (2)$$

where k = 1 for i = 1. 2. 3... for experiments 1 through 9 and refer to the sequence following data pre-processing and the comparability sequence, respectively. Table 4 presents the gray relational generation and deviation results. Equation 3 was used to determine the comparability sequence and the reference sequence's deviation sequence:

$$\Delta_{0i}(k) = |x_0^{x}(k) - x_i^{x}(k)| \quad (3)$$

Table 3: Results of the Taguchi experiment(L9)

S/No	%wtCNTs		%wtPWSnp	Stirring speed	Stirring time	Porosity(%)	Hardness Values(HV)	Compressive strength(MPa)
1	1		1	1	1	0.12	87.56	245.67
2	1		2	2	2	0.12	89.01	268.23
3	1		3	3	3	0.15	91.50	289.45
4	2		1	2	3	0.18	98.32	345.78
5	2		2	3	1	0.25	99.26	367.8
6	2		3	1	2	0.34	97.90	355.89
7	3		1	3	2	0.3	105.89	401.89
8	3		2	1	3	0.290	116.8	410.67
9	3		3	2	1	0.30	100.89	398.76

Equation (4) was used to calculate the Grey Relational Coefficients (GRC) for the output characteristics.

$$\zeta_1(K) = \frac{\Delta_{mm} + \zeta\Delta_{\max}}{\Delta_{0i}(k) + \zeta\Delta_{\max}} \quad (4)$$

The calculated deviation from the normalized S/N value is represented by Δoi(k), and the values of the Δmax maximum and Δmin minimum normalized S/N ratios for each of the three output characteristics are typically 1 and Δmin minimum, respectively. ξi(k) is the grey relational coefficient, ξ is the distinguishing or identification coefficient which lines within 0 ≤ ξ ≤ 1, and ξ equal to 0.5 was adopted in this research. The average of the GRC for each performance criteria yields the GRG. The GRG, as shown in Equation 5, serves as the foundation for the overall assessment of the various performance parameters.

$$r_1 = \frac{1}{n}\sum_{k=1}^{n}\zeta_1(k) \quad (5)$$

where n is the number of performance criteria, and Yi is the GRG for the Ath experiment. Consequently, the corresponding experimental result was closer to the ideal normalized value when the GRG was higher. The results of the GRC and GRG are presented in Table 5

Table 4: Grey relational generation and deviation

S/NO	**Grey relational generation**			**DOI**		
	Hardness values	**Compressive strength**	**porosity**	**Hardness values**	**Compressive strength**	**porosity**
1	**0**	**0**	**1**	**1**	**1**	**0**
2	0.049589603	0.136727273	**1**	0.950410397	0.863272727	**0**
3	0.134746922	0.265333333	0.863636364	0.865253078	0.734666667	0.136363636
4	0.367989056	0.606727273	0.727272727	0.632010944	0.393272727	0.272727273
5	0.400136799	0.740181818	0.409090909	0.599863201	0.259818182	0.590909091
6	0.353625171	0.668	**0**	0.646374829	0.332	**1**
7	0.626880985	0.946787879	0.181818182	0.373119015	0.053212121	0.818181818
8	**1**	**1**	0.227272727	**0**	**0**	0.772727273
9	0.455882353	0.927818182	0.181818182	0.544117647	0.072181818	0.818181818

Table 5: Grey relational coefficient and Grey Relational Grade (GRG)

S/NO	Grey relational coefficient			Grey Relational Grade (GRG
	Hardness values	Compressive strength	porosity	
1	0.75	**0.75**	**0.25**	0.583333333
2	0.725205198	0.681636	**0.25**	0.552280521
3	0.682626539	0.617333	0.318181818	0.539380564
4	0.566005472	0.446636	0.386363636	0.466335157
5	0.549931601	0.379909	0.545454545	0.491765079
6	0.573187415	0.416	0.75	0.579729138
7	0.436559508	0.276606	0.659090909	0.457418826
8	0.25	0.25	0.636363636	0.378787879
9	0.522058824	0.286091	0.659090909	0.489080214

3.2 Testing Friction properties of the prototype disc and Brake pad

In accordance with JASO C406-82, the friction properties of the developed brake disc were tested using a brake pad. The brake pad with minimal film deposition on the surface, which is frequently used for testing conventional cast iron brake discs, was the one chosen for the frictional analysis [Ezechukwu, 2025; Hiroaki, 2002]. The developed brake disc was repeatedly used in the braking operation with the brake pad of 75km/h and deceleration of 3.5m/s before braking at 130°C. The coefficient of friction was determined, and the wear rate of the disk and brake pad was measured. Figure 2 displays the results of the coefficient of friction with braking times, and Figure 3 shows the wear rate of the pad and disc. It was discovered that the wear rate and the obtained coefficient of friction for both materials are similar. The developed brake disc has been shown to compare favorably with the conventional brake disc.

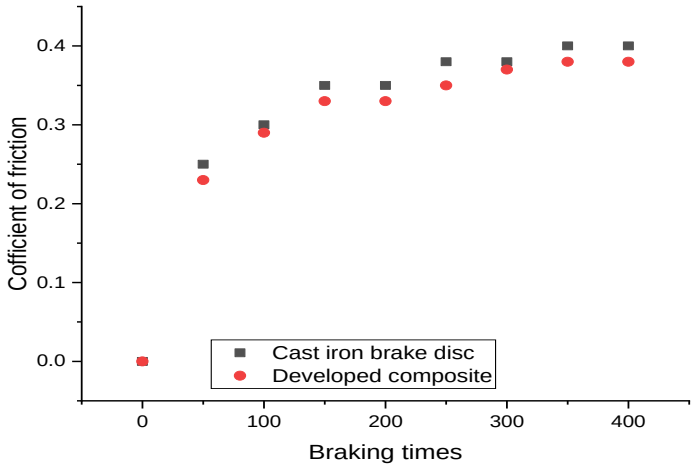

Figure 2: Variation of coefficient of friction with braking times

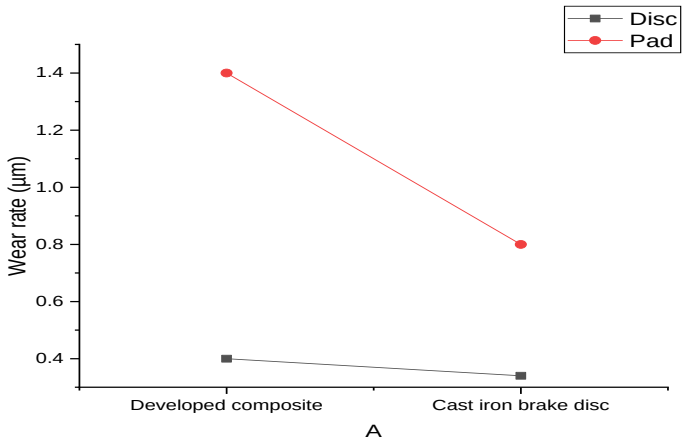

Figure 3: Variation of wear rate with samples

3.3 Structural simulation analysis of the developed disc brake based

3.3.1Geometric model

The displacement, Von mises stress, and factor of safety, as shown in Equations 1-3, were used to determine the stress analysis of the developed brake disc using the composite on a Toyota Corolla brake disc sample in accordance with standard procedure (Figure 4).

$$\sigma_v = [0.5((\sigma_1 - \sigma_2)^2 + (\sigma_2 - \sigma_3)^2 + (\sigma_3 - \sigma_1)^2)]^{0.5} \quad (6)$$

$$Eqs = (\frac{4}{3}.\sigma_v)^{0.5} \quad (7)$$

$$F_s = \frac{\sigma_v}{W_s} \quad (8)$$

where: σv =Von mises stress, σ1 σ2σ3 = principal stresses, EqS = Equivalent strain, Ws= workable stress, Fs= factor of safety

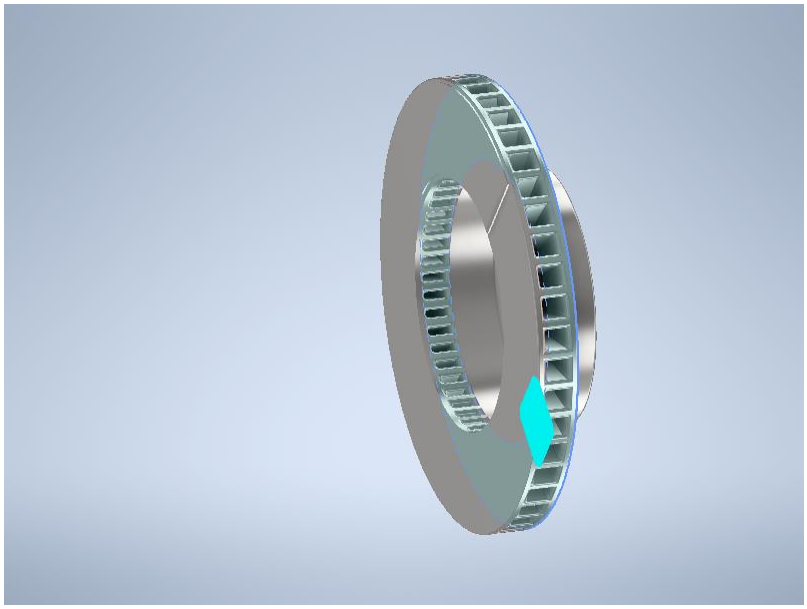

Figure 4 displayed the three-dimensional view model of the brake disc

3.3.2 Meshing

In the disc brake, there are many chamfers and grooves that increase heat dissipation spokes between the internal structure and double-layer discs. The restraining of the x, z-direction, and center location in y-displacement were the boundary conditions applied in this stress analysis. Minimum element sizes of 0.2 0.05 shells, maximum turning angle of 60°, fraction model diameter 0.1, and grading factor of 1.5 were used for the meshing. The finite-element model considerations of 1202 elements and 686 nodes were used.

3.3.3 Brake disc strength analysis

The outer and inner caliper bodies are normally used during the braking operation. The fluid of brake pressure is normally transmitted from the pistons and brake pads. The force from the bolts fixed in between the axle, brake pads, the magnitude of the brake fluid pressure, and the caliper body have a relationship with the external force of the vehicle speed and brake pedal. In this work, a car traveling at 100 km/h and the contact friction force (torque) of the friction surface of the disc brake and friction pad were used for the simulation. After substituting the pressure, the pressure brake pad and disc (Nmax) = 19096 N was obtained; these values were used in the simulation.

$$N = P_1 S_1 = P_1 \Pi d_i x 0.25 \quad (9)$$

$$T_f = 2fNR \quad (10)$$

Where: N= pressing force of the brake disc and friction pad on the P_1=the hydraulic pressure(MPa); S_1: pad area(cm^2); d_1: diameter of the piston(cm) f: = coefficient of friction, R= radial dimension(cm)

3.3.4 Restraint and Load Determination

When applying the load, the disc brake mainly acts on the brake pad, as displayed in Figure 5. Defining constraints, the center hole of the brake disc, X constraints on the outer and, inner and end surfaces of the disc, then Y and Z constraints on the friction surface of the friction lining and brake disc as shown in Figure 5.

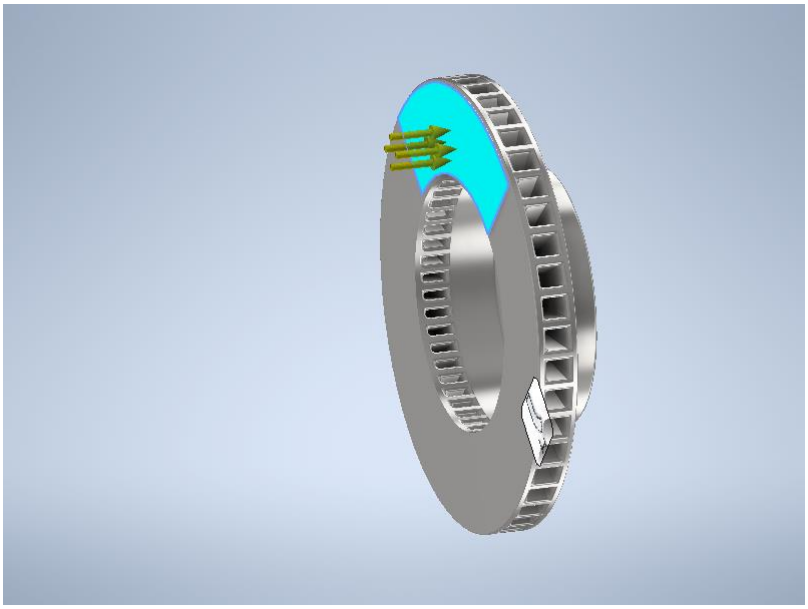

Figure 5 Load position.

3.4 Simulation results

The analysis of the structural strength of the brake disc after the simulation, Figures 6-8, displayed results of modal analysis, stress solution, and deformation cloud diagram. It was observed that the maximum stress of the brake disc during the braking process is 15.8402 MPa, and the compressive strength of the brake disc is 410 MPa, so the brake

disc fully meets the strength requirements. It can be seen from the deformation cloud diagram that the maximum deformation of the brake disc during braking is 0.00172654 mm, and the closer the center is, the smaller the deformation. From the observation of the linear structural analysis, the Von stress was lower compressive strength of the developed brake disc; this shows that high-strength brake discs give a minimum factor of safety of 7.58 and 15. It can be concluded that the strength and safety factors are within the recommended standard for brake disc applications.

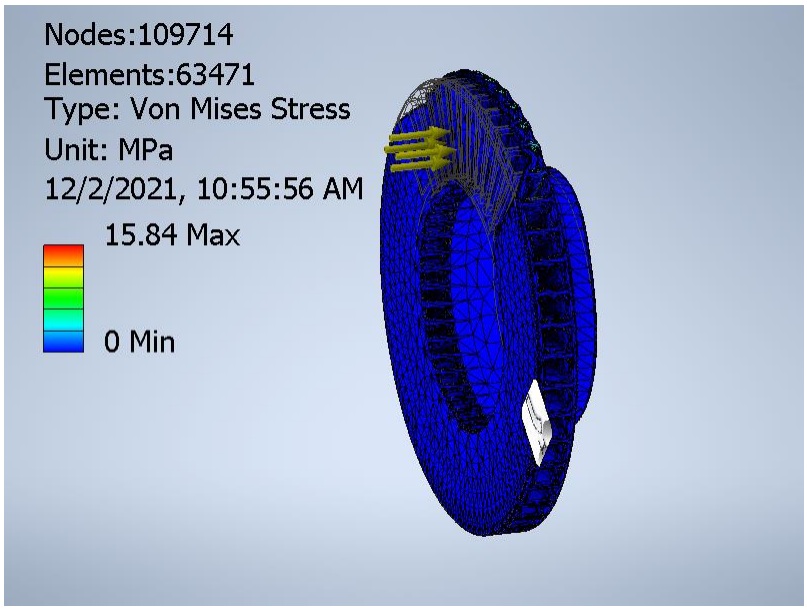

Figure 6: The Von Mises stress

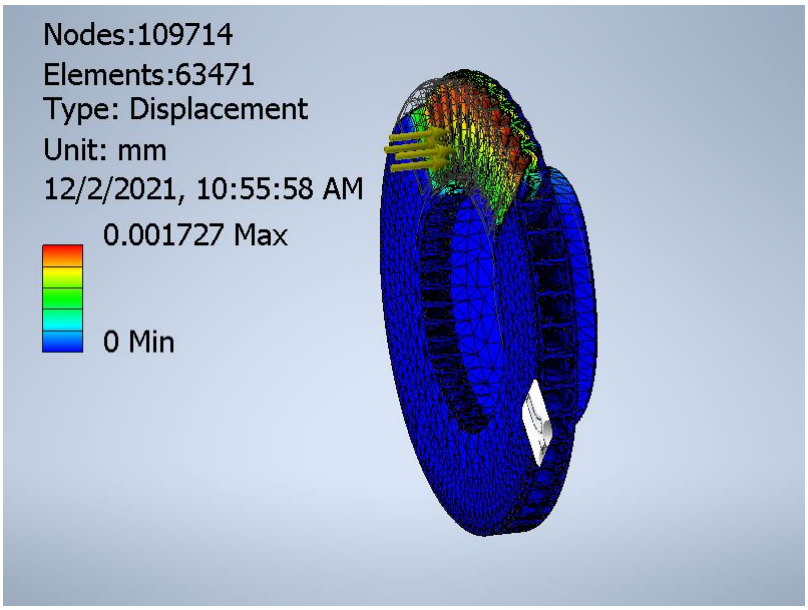

Figure 7: the displacement

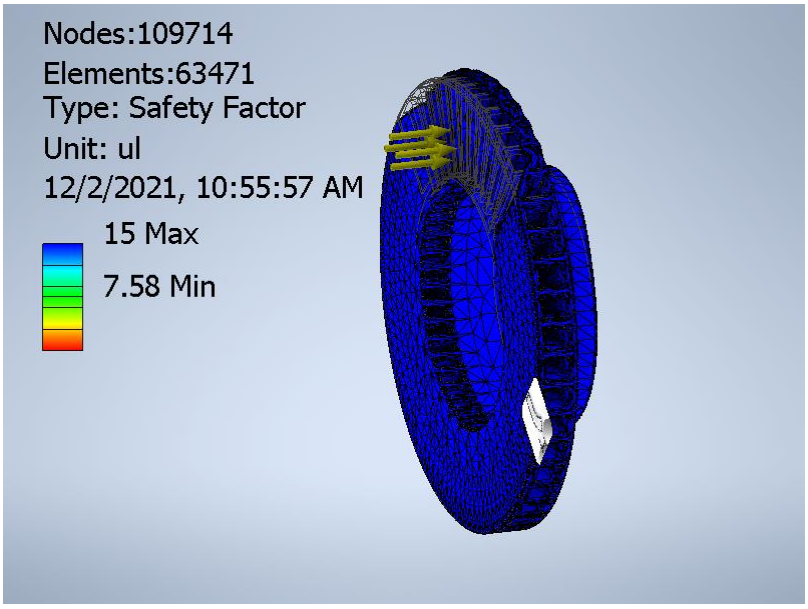

Figure 8: the factor of safety

4. Conclusions

The study provided new information regarding the structural performance of a newly developed aluminum alloy composite for brake disc applications that uses PWSnp and CNTs produced from RH. The following can be produced during the research: RH derived from CNTs, waste beverages, and periwinkle shells can all be successfully used to create nanocomposites for use as structural materials. The highest stress of the brake disc obtained during the braking process is 15.8402 MPa, and the compressive strength of the brake disc is 410 MPa; therefore, the brake disc fully meets the strength requirements. It can be seen from the deformation cloud diagram that the maximum deformation of the brake disc during braking is 0.00172654 mm, and the closer the center is, the smaller the deformation. From the observation of the linear structural analysis, the Von stress was lower compressive strength of the developed brake disc; this shows that high-strength brake discs give a minimum factor of safety of 7.58 and 15. It can be concluded that the strength and safety factors are within the recommended standard for brake disc applications.

Funding: The authors declare that no funds, grants, or other support were received during the preparation of this manuscript.

Author contributions: All the authors contributed to the development of the work. All authors read and approved the final manuscript.

Declaration of interests. The authors declare that none of the work described in this study could have been influenced by any known competing financial interests or personal relationships.

Competing interests: The authors declare no competing interests.

Data Availability The authors confirm that the data supporting the findings of this study are available within the article.

References

[1] Braide T. K, Chidozie C N, Vincent C E and Remy U. (2023). Multi objective optimization of novel Al-Si-Mg nanocomposites: A Taguchi-ANN-NSGA-II Approach, *Journal of Engineering Research, 2023*, ISSN 2307-1877, https://doi.org/10.1016/j.jer.2023.10.008. (https://www.sciencedirect.com/science/article/pii/S2307187723002687)

[2] Braide, T.K., Nwobi-Okoye, C.C. & Ezechukwu, V.C. (2022). Taguchi-Grey multi-response optimization of wear parameter of new nanocomposite formulation of Al–Si–Mg alloy reinforced with synthesis carbon nanotube and periwinkle shell nanoparticles. *Int J Adv Manuf Technol* 120, 8363–8375 (2022). https://doi.org/10.1007/s00170-022-09163-7

[3] Braide T.T., Nwobi-Okoye C.C., and Ezechukwu V.C. (2022). Microstructural and Electrochemical study of Value-added Al-Si-Mg alloy reinforced with synthesis carbon nanotube and periwinkle shell nanoparticles for brake disc application, Chemical

Data Collections, 39, 2022, 100878, ISSN 2405-8300, https://doi.org/10.1016/j.cdc.2022.100878. (https://www.sciencedirect.com/science/article/pii/S2405830022000519)

[4] Dhanalakshmi S, Mohanasundararaju N and Venkatakrishnan PG (2018). Optimization of friction and wear behavior of Al7075-Al2O3-B4C metal matrix composites using Taguchi method. Mater Sci Eng 314:012025

[5] Ezechukwu, V.C., Braide, T.K. and Nwobi-Okoye, C.C. (2024). Multi-Response Optimization of Stir Casting Parameter of New Nanocomposites Formulation of Al-Si-Mg Alloy Reinforced with Synthesis Carbon Nanotube and Periwinkle Shell Nanoparticles via Taguchi-Grey Approach. *International Journal of Science and Engineering Invention.* 10, 10 (Dec. 2024), 71–81. DOI:https://doi.org/10.23958/ijsei/vol10-i10/276.

[6] Ezechukwu, V, C. (2024). Hybridization Effect on Thermo-mechanical Behaviour of Epoxy/breadfruit Seed Shell Ash Particles and Momordica Angustisepala Fiber Composites for High- temperature Devices Application. Proceedings of the IRE. 7. 2456-8880. https://www.irejournals.com/formatedpaper/1705783.pdf

[7] Ezechukwu, V. C., Onyenanu, I. U. ., Ayadinuno, G. ., & Agwaziam, J. O. (2025). Structural simulation analysis of the developed hybrid of Momordica angustisepala fiber and Breadfruit seed-shell particles composites Bolted Flanges. *IPS Journal of Engineering and Technology*, 1(1), 13–20. https://doi.org/10.54117/ijet.v1i1.2.

[8] Ezechukwu, V.C., Nwobi-Okoye, C.C., Atanmo, P.N., and Aigbodion, V.S. (2020). Wear performance of value-addition epoxy/breadfruit seed shell ash particles and functionalized Momordica angustisepala fiber hybrid composites. Revue des Composites et des Matériaux Avancés-*Journal of Composite and Advanced Materials*, 30, 5-6, 195-202. https://doi.org/10.18280/rcma.305-601

[9] Ezechukwu, V.C., Nwobi-Okoye, C.C. & Atanmo, P.N. (2020). Surface modification of Momordica angustisepala fiber using temperature-activated amino-functionalized alkali-silane treatment. Int J Adv Manuf Technol 109, 1397–1407. https://doi.org/10.1007/s00170-020-05697-w

[10] Hiroaki N, & Kenji K, (2002). Development of aluminum metal matrix composites (Al-MMC) brake rotor and pad. JSAE Review, 23, 365- 370.

[11] Nnaji, N B., Kennedy, C., Ezechukwu, V C. (2024). Characterization of Pig Bone Ash and Hamburger Seed Shell Wastes from Umuahia, Abia State, NIGERIA. *International Research Journal of Modernization in Engineering Technology and Science (IRJMET)*:06/Issue:12. e-ISSN: 2582-5208. DOI: https://www.doi.org/10.56726/IRJMETS64861

[12] Nnaji, N. B., Owuama, K. C., Ezechukwu, V. C (2024). Microstructural and Chemical Analysis of Polypropylene/Pig-Bone-Ash/Hamburger Seed Shell Composite. *International Journal of Progressive Research in Engineering Management and Science (IJPREMS)* e-ISSN: 2583-1062, Vol. 04, Issue 12, pp: 901-913, DOI: https://www.doi.org/10.58257/IJPREMS35744

[13] Natarajan, N., Vijayarangan, S., & Rajendran, I. (2006). Wear behavior of A356/25SiCp aluminum matrix composites sliding against automobile friction material. Wear, 261(7-8), 812–822. doi: 10.1016/j.wear.2006.01.011

[14] Onyenanu, I. U., & Nwigbo, S. C. (2021). Optimization of aluminium metal matrix composite (AMMC) for use in automobile brake disc. Int. J. Eng. Res. Technol, 10.

[15] Onyenanu, I. U., Ukwu, N. O., Ezechukwu, V. C., Onyenanu, I. M., & Nwadiuto, C. J. (2024). Modelling and Optimization of Banana/Plantain Fiber Extraction Systems through Dimensional Analysis. *International Journal of Applied and Natural Sciences*, *2*(2), 40–52. https://doi.org/10.61424/ijans.v2i2.161

[16] Obinwa, C C., Ezechukwu, V C., Nwosu, A W. (2024). Optimization and Analysis of Mechanical Properties (Tensile Strength) in a developed Plantain Hybrid Fibre Reinforced Composite (PHFRC). *International Journal Of Engineering Research And Development*. e- ISSN: 2278-067X, p-ISSN: 2278-800X, 20, 12, 109-119 http://www.ijerd.com/

[17] Onyenanu, I. U., & Nwigbo, S. C. (2021). Optimization of aluminium metal matrix composite (AMMC) for use in automobile brake disc. *Int. J. Eng. Res. Technol*, *10*.

[18] Venkatachalam, G., & Kumaravel**,** A. (2017). Mechanical Behaviour of Aluminium Alloy Reinforced with Sic/Fly Ash/Basalt Composite for Brake Rotor. *Polymers and Polymer Composites, 25*(3), 203–208. doi:10.1177/096739111702500304